Magnetic Ordering of Defects in a Molecular Spin-Peierls System

Adam Berlie

E-mail: adam.berlie@stfc.ac.uk
ISIS Neutron and Muon Facility, Science and Technology Facilities Council, Chilton, Oxfordshire, OX11 0QX, United Kingdom.
RIKEN Nishina Center for Accelerator-Based Science, 2-1 Hirosawa, Wako, Saitama 351-0198, Japan.
Department of Physics, Durham University, South Road, Durham, DH1 3LE, United Kingdom.

Ian Terry

Department of Physics, Durham University, South Road, Durham, DH1 3LE, United Kingdom.

Stephen Cottrell

ISIS Neutron and Muon Facility, Science and Technology Facilities Council, Chilton, Oxfordshire, OX11 0QX, United Kingdom.

Francis L. Pratt

ISIS Neutron and Muon Facility, Science and Technology Facilities Council, Chilton, Oxfordshire, OX11 0QX, United Kingdom.

Marek Szablewski

Department of Physics, Durham University, South Road, Durham, DH1 3LE, United Kingdom.

Content & Services Team

June 2016

Abstract. With interest in charge transfer compounds growing steadily, it is important to understand all aspects of the underlying physics of these systems, including the properties of the defects and interfaces that are universally present in actual experimental systems. For the study of these defects and their interactions a spin-Peierls (SP) system provides a useful testing ground. This work presents an investigation within the SP phase of potassium $TCNQF_4$ where anomalous features are observed in both the magnetic susceptibility and ESR spectra for temperatures between 60 K and 100 K. Muon spin spectroscopy measurements confirm the presence of these anomalous magnetic features, with low temperature zero-field data exhibiting

the damped oscillatory form that is a characteristic signature of static magnetic order. This ordering is most likely due to the interaction between structurally correlated magnetic defects in the system. The critical behaviour of the temperature dependent muon spin rotation frequency indicates that a 2D Ising model is applicable to the magnetic ordering of these defects. We show that these observations can be explained by a simple model in which the magnetic defects are located at stacking faults, which provide them with a 2D structural framework to constrain their interactions.

Introduction

When trying to understand the underlying physics of materials it is important to study the role of magnetic defects and interfaces [1, 2, 3]. One area where there has been a wealth of research activity is organic magnetism, with much work conducted on charge transfer systems [4, 5, 6] although defect properties of these compounds have not received much attention. In order to focus specifically on the defect magnetism, a good strategy is to choose a system in which the background contribution is non-magnetic, which can be achieved by using a spin-Peierls (SP) system. Below the SP transition temperature (T_{SP}) the magnetic entities are dimerised and fall into a singlet ground state, thus the majority of the material does not contribute to the magnetic susceptibility [7]. The alkali metal TCNQ (7,7,8,8-tetracyanoquinodimethane) compounds are 1:1 salts that undergo SP transitions red through the dimerisation of TCNQ anions depending on the cation used [8, 9, 10, 11]. Other notable examples include the 1:2 TCNQ salts [12, 13, 14] as well as inorganic SP materials such as $CuGeO_3$ [15, 16, 17], $TiPO_4$ [18] and NaV_2O_5 [19]. Using non-magnetic Zn doping within the $CuGeO_3$ system, one is able to change the magnetism as well as induce an antiferromagnetic or a spin glass state below T_{SP} [20, 21, 22, 23, 24]. This effect is one example of how defects interact with each other and the underlying SP phase, which is a starting point that can be extended for the understanding of other types of materials.

Potassium TCNQ is a simple, well known SP compound that undergoes an SP transition at 395 K [25, 26]. Furthermore, this transition can be tuned by replacing protons with fluorine atoms on the quinoidal ring of TCNQ using $TCNQF_4$ ($TCNQF_4$ = 2,3,5,6-tetrafluoro-7,7,8,8-tetracyanoquinodimethane) where a shift in T_{SP} to 160 K is observed [27]. $TCNQF_4$ is a stronger acceptor than TCNQ as the F atoms can draw an increased amount of electron density into the quinoidal structure. This results in a rapid synthesis, which makes for purer samples, but inevitably causes structural defects. Within this $KTCNQF_4$ compound the defects states are due to non-dimerised $TCNQF_4$ anions and an anomalies in both red the temperature-dependent magnetic susceptibility, $\chi(T)$, and ESR data at 90 K are taken to be evidence for the interactions between such defects. Using a more sensitive probe of weak magnetism, muon spin relaxation (μSR), we are able to eliminate contributions from the background SP phase, Curie-type paramagnetism and diamagnetism to study only the defect magnetism in

more detail and we find that critical the behaviour associated with magnetic ordering of defects can be described by the 2D Ising model.

Experimental Techniques

The sample was made by refluxing potassium iodide and $TCNQF_4$ in acetonitrile and the resultant precipitate was washed with diethylether. The precipitate forms a powder that is comprised of small needle like crystals that are visible under an optical microscope and 10's of microns in size. It is likely that the long axis of the needle is the stacking planes of the TCNQ molecules. Electron Spin Resonance (ESR) experiments were conducted using a Bruker BioSpin system with an X-band microwave source and a He gas cryostat capable of reaching temperatures down to approximately 5 K. Magnetic data were collected using a Quantum Design MPMS with an applied field of 50 kG. Muon spin relaxation experiments were conducted at the ISIS neutron and muon source using the ARGUS, EMU and MUSR spectrometers. In a μSR experiment, spin polarised positive muons (μ^+) are implanted in the sample. redThe muons have a lifetime of 2.2 μs and they decay to produce a positron and an antineutrino, the direction of the positron emission being related to the muon's spin at the time of the decay [29]. On implantation, the moment of the muon will precess in the presence of internal magnetic fields, the precession having a single frequency if all the muons experience the same internal magnetic field. However, if the internal field is inhomogeneous there will be a range of muon spin rotation frequencies as a consequence of the field distribution. The field distribution will become more broad depending on the level of disorder or dynamical behaviour of the nuclear and electronic moments. redThe field distribution causes a depolarization of the spins of the muons which can be observed by measuring the time dependence of the asymmetry in the decay of the muon ensemble in a forward and backward detector banks. The asymmetry is then defined as

$$a_0 = \frac{N_B - N_F}{N_B + N_F}, \tag{1}$$

where $N_{F,B}$ is the number of counts in the forward and backward detector banks. Measuring the relaxation of the asymmetry can therefore be used to understand the static magnetic field distributions and magnetic fluctuations within the system. Application of a longitudinal field (LF) along the initial muon polarisation direction can be used to decouple static components allowing one to study the interaction between the muon and local magnetic moments.red More information on muon spectroscopy can be found within references [29, 30]. Since μSR is a local, sensitive probe of weak internal fields and magnetic fluctuations on the MHz time scale, it is useful for studying systems where the magnetic order is dilute and a large field may need to be applied when performing magnetic susceptibility measurements to increase the response. Since experiments can be performed in zero-field or a very small longitudinal field, this also means that the diamagnetic response of the sample is very small and, consequently provides a negligible contribution to the μSR signal. It should also be noted that the

paramagnetic signal is also negligible as the dynamics are extremely fast and so the muon is in the motionally narrowed state. On the ARGUS and EMU spectrometers a full redasymmetry in positron emission following the muons' decay is approximately 23% and on MUSR, approximately 25%. red From knowing the relaxing asymmetry of each component, one can work out a total percentage of muons that are dephased by each component, which one could consider similar to a number density.

Results and Discussion

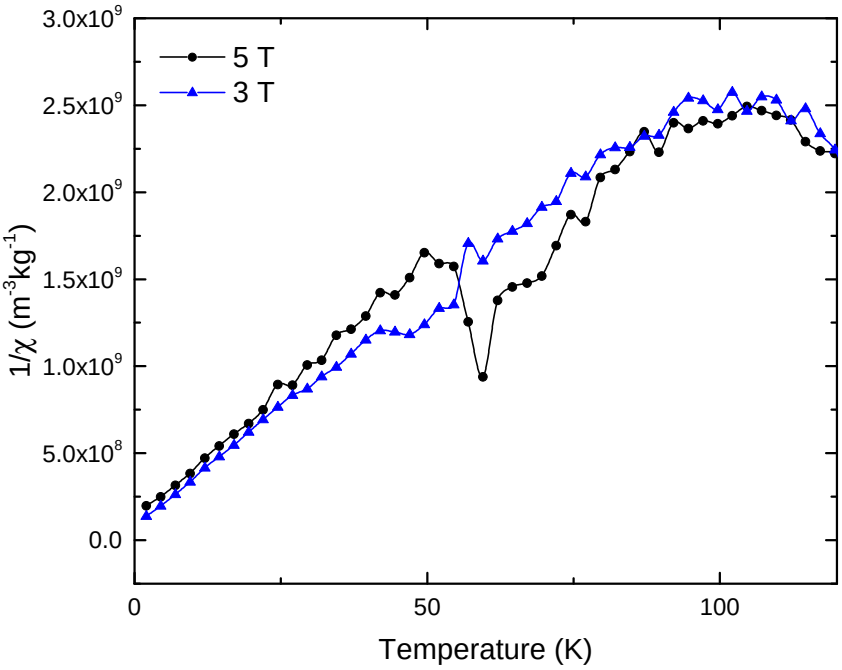

Figure 1. Inverse magnetic susceptibility at low temperatures collected in 30 and 50 kG. The anomaly is only present in the 50 kG data where the large field blows up the component enough to see evidence of a T_C at approximately 60 K.

Magnetic susceptibility measurements made below T_{SP} redexhibited both a paramagnetic response (Curie tail) below 30 K and an anomaly between 60 - 80 K occurred only in the 50 kG data (see Figure 1). The low temperature paramagnetic response is likely to be a consequence unpaired electrons situated on non-dimerized TCNQF4 molecules arising from, say, vacancies in the crystal structure. The 60K anomaly may be a consequence of some of these paramagnetic defects being in close enough proximity to allow the exchange coupling of the $TCNQF_4$-bound radical spins. A high field of 50 kG was needed to make the magnetic response of the exchange-coupled defects more visible, using a lower field was not enough to blow up the component of interest from the diamagnetic background. A separate diamagnetic susceptibility was subtracted from both data sets where the values were estimated to be -2.24×10^{-8} and -2.27×10^{-8} m^3kg^{-1} for the 50 and 30 kG data respectively, which caused the

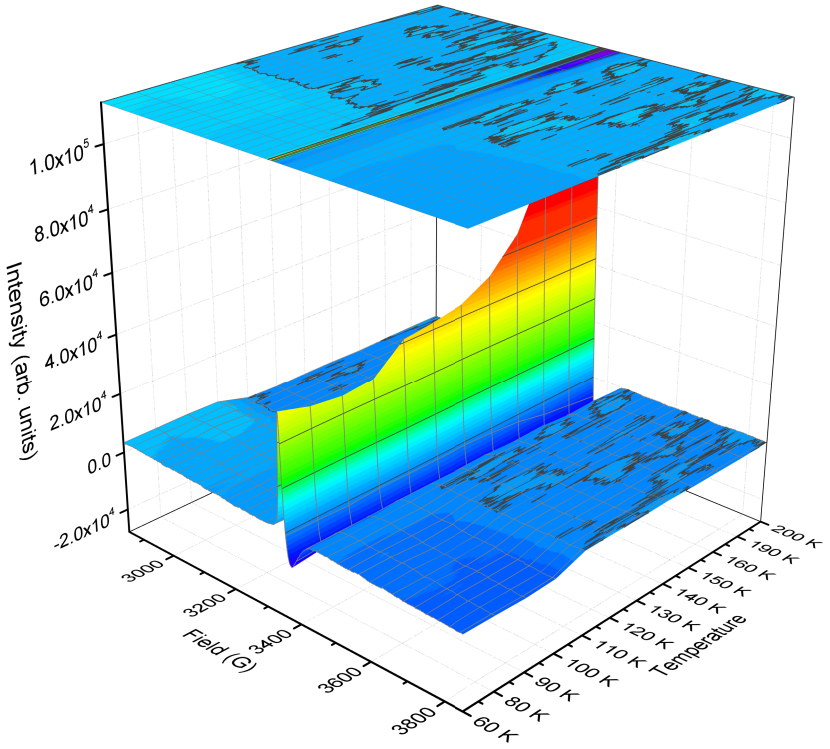

Figure 2. ESR raw data at between 60 and 200 K showing the anomaly at ∼90 K. This anomaly is thought to be due to interactions between these defect states. *Note: The temperature axis is non-linear.*

two curves to fall onto one another. The fact that these diamagnetic susceptibilities were estimated to be different implies that there is another effect compensating for this difference. From the shape of the peak within the 50 kG curve, it is reminiscent of an antiferromagentic transition and so one could postulate that these defects couple antiferromagnetically

In a further attempt to pin down information on the defect magnetism, a temperature dependent ESR experiment was conducted. Below T_{SP} one expects the contribution from the majority of TCNQ anions associated with the SP transition to disappear and thus only contributions from defects or other magnetic centres should be present as seen in Ni doped $CuGeO_3$ compound where at low temperatures an ESR peak from the Ni(II) was revealed [28]. Raw data over the entire temperature range can be seen in the supplementary information where above 150 K there is an increase in the peak intensity that corresponds to the SP transition. At 90 K there is an anomaly in the raw data (see Figure 2), which is a similar temperature to the onset of the Curie-Weiss behaviour in the magnetic data shown in Figure 1 suggesting that the two are linked. The g-factor is very close to 2, indicating an orbitally quenched $S = 1/2$ defect red is responsible for the signal. The line-shape is strongly asymmetric and this may be an indication that there are various underlying peaks or a complicated spin-lattice relaxation mechanism.

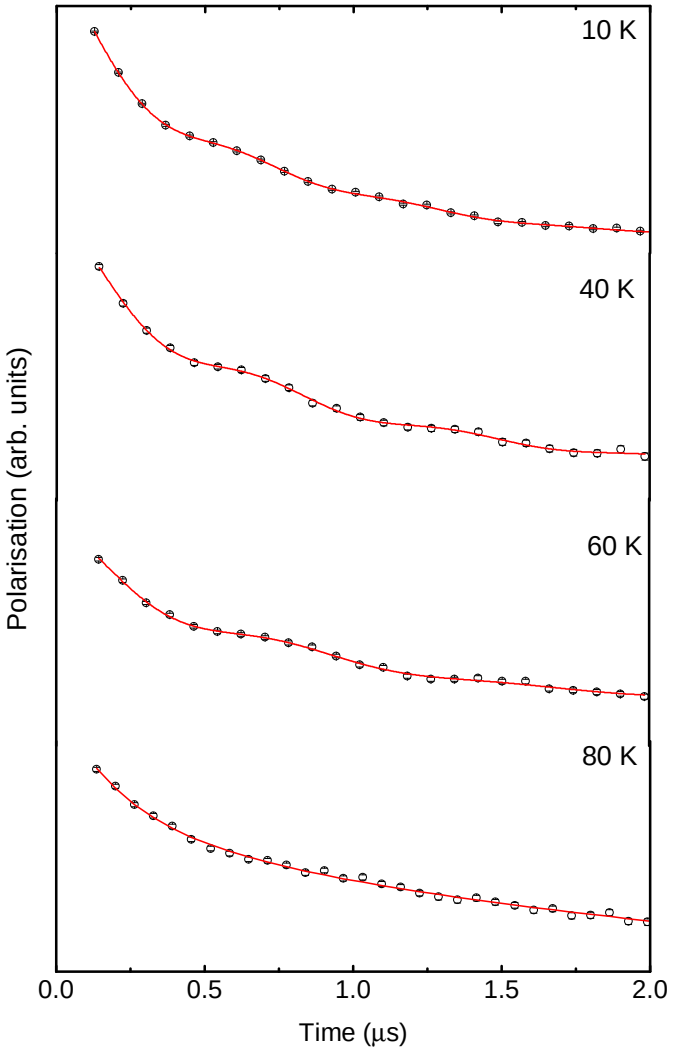

Figure 3. Short time μSR raw data for $KTCNQF_4$ showing the damped oscillation at selected temperatures, data are offset for clarity. The red lines show fits to the data using equation 1. redNote that the 10 K spectrum was collected on the MUSR spectrometer rather then EMU due to beam time scheduling.

The effect in both the magnetic susceptibility and ESR data is very weak and at the limits of both techniques. redSince μSR is an excellent probe of weak, local magnetic fields it presents some significant advantages for studying the static and dynamic properties of the defect states.The sensitivity of this technique is a consequence of the fact that muons can implant close to local magnetic moments and experience their local dipolar magnetic fields. The high temperature behaviour through T_{SP} of the muon relaxation has been previously studied [27] and so here, we only focus on the low temperature behaviour. The relaxation at low temperatures is complex as there are many different relaxation mechanisms but at short times one is able to resolve a heavily damped oscillation, a signature of static magnetic moments, on a strongly relaxing background. redSince the sample was a powder, an average over all orientations is

observed, where in the case of μSR, the muon precesses around fields perpendicular to its initial polarisation. The amplitude of the precession/oscillatory signal will account for 2/3 of the asymmetry of the muon decay associated with this component, which arises due to static magnetic moments orientated along axis that are transverse to the initial muon polarisation.

The zero-field raw data are shown in Figure 3 where one can clearly see the oscillatory signal from the muon spin rotation, however at 80 K it is lost and so this can be considered as an upper limit for T_{N}. Between 50 and 70 K all data were fit using the equation:

$$G(t) = A_1 cos(\omega t + \phi) \cdot \exp(-\lambda_1 t) + A_2 \exp(-\lambda_2 t) + A_{bg}, \tag{2}$$

where ω is the frequency (in rad s^{-1}), ϕ is the phase offset, λ_n is the muon spin relaxation rate, A_n is the asymmetry of each component (note; bg is the background term). The asymmetry of the oscillatory component is very low and approximately 1.5% on average, the relaxation rate is fast (> 1 $\mu\mathrm{s}^{-1}$) and in all cases the asymmetries and relaxations (A_2, λ_2 and A_{bg}) are there to account for the relaxing background. red The percentage of defects can be calculated from the ratio of the relaxing asymmetry to the full asymmetry, i.e. $1.5/23 \times 100 = 6.5\%$, which is of the same order of magnitude as the number density calculated from the magnetic susceptibility. However, if the defects sites are electron rich, then this might promote a favourable stopping site for the μ^+, even if it is an incredibly reddilute state and this may result in an over-estimate of the percentage of defects. The frequency of the oscillation (ν) is related to the internal field (B_{Int}) at the muon site by $\nu(\mathrm{MHz}) = \gamma_\mu B_{\mathrm{Int}}$, γ_μ is the muon gyromagnetic ratio. red The presence of an oscillatory signal is an indication of static, ordered magnetic moments on the muon time scale, but there is also a large damping of this signal. This damping or field distribution was modelled with an Lorentzian distribution, which could mean the magnetic moments associated with the defects are dilute and inhomogeneously distributed throughout the sample.

At low temperatures ($\leq$40 K), an additional component must be added to the fitting function that accounts for the formation of an F-μ^+-F state in order to get a good fit to the raw data. The F-μ^+-F state has been previously reported many times[32, 33] and can be a useful way to determine muon stopping sites. In our case, the F-μ^+ distance was fixed at 0.12 nm, but again the asymmetry is very low accounting for redapproximately $0.5 \pm 0.1\%$ total asymmetry, or $\sim$2% of the total amount of muons , showing it is a minor component. From the F-μ^+ distance, one can begin to get an idea of the stopping site associated with this state which is shown in Figure 4.

The temperature evolution of the frequency of the oscillatory component can be used to gain a value T_{C} and also to model the critical nature [35] of the transition in zero-field. The frequency is related to the critical exponent (β) by

$$\nu(T) = D(1 - T/T_{\mathrm{C}})^{\beta}, \tag{3}$$

where D is the pre-exponent or the frequency factor at $T = 0$. It should be emphasised that T_{C} from μSR and the magnetic susceptibility/ESR measurements will

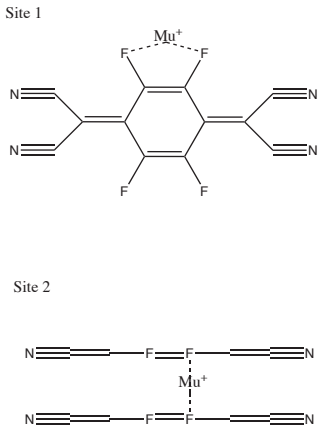

Figure 4. Muon sites that may correspond to the F-μ^+-F state. An F-μ^+ distance of 0.12 nm could be due to the muon stopping at site 1.red In the case of a $TCNQF_4$ charge transfer salt[34], the calculated F-F distance is 0.27 nm and if the muon stops half way between the two F atoms this would result in an F-μ^+ distance of 0.13 nm, which is close the what we observe.

be different as all these measurements have inherent time scales that are vastly different. From the raw data in Figure 3, T_C is placed between 70 and 80 K, therefore T_C must be constrained to be between these temperatures. As a good estimate, D can also be fixed at 1.7 MHz (125 G) and then one has only to consider both T_C and β when modelling the data. A rough fit produces a $T_C = 71.0 \pm 0.5$ K and these values can be used to simulate what the transition would look like with different values of β. Within Figure 5 different curves have been simulated for different critical exponents when $\beta = 0.125$, 0.2 and 0.326 and using the values of D and T_C already discussed. It is apparent that the clearest agreement comes from the critical exponent, $\beta = 0.125$, which corresponds to a 2D Ising model and since the Curie-Weiss behaviour has a negative value of θ, this may be an indication that antiferromagnetic exchange dominates. For a 3D Heisenberg system, where $\beta = 0.326$, the increase in the frequency is too shallow and so is not a realistic model. Keeping the value of D fixed also manages to capture the 20 K point, but it should be considered that this is well outside the critical region, however other work has shown critical scaling fits down to low temperatures [35].

A longitudinal field (LF) sweep is a useful way of studying the different magnetic environments or the decoupling of the muon from its internal environment. Across all field ranges at 30 K the data were fit with a single exponential relaxation that results (see the inset of Figure 5) in a relaxation rate (λ) with a peak at approximately 109 G, which is of the same order of magnitude as that computed from D. This is likely a good representation of the internal field at the muon stopping site where increasing LF decouples more components and the flat relaxation achieved at higher fields means the muon is completely decoupled from its magnetic environment within the sample. The low field (<50 G) behaviour is due to a decoupling of the muon relaxation from the dipolar fields of the nuclear moments. The increase in the relaxation is not expected but may be a feature of the superposition and convolution of relaxations from inequivalent

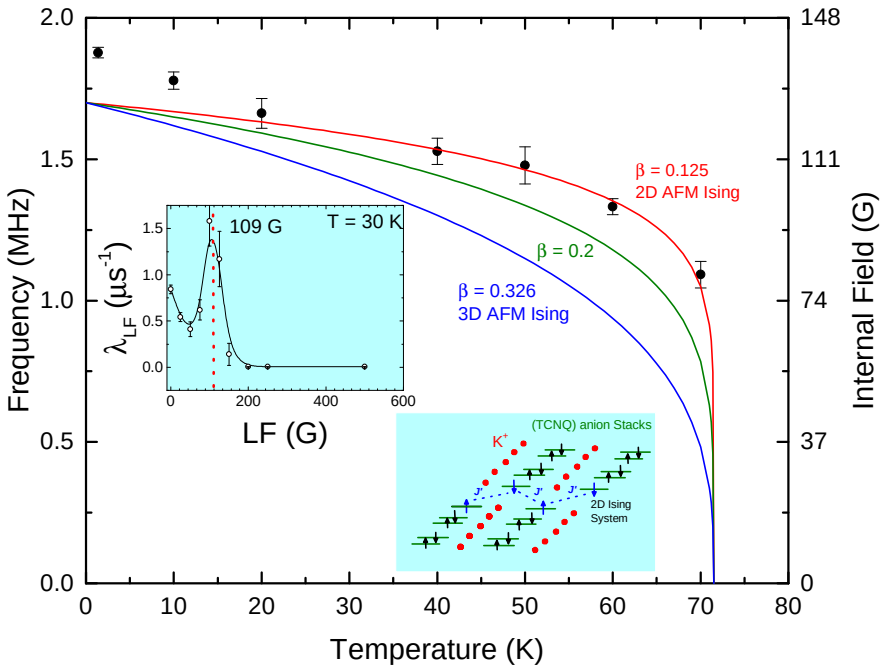

Figure 5. Temperature dependence of the frequency, ν, related to the internal field that is coupled to the muon that is a consequence of the ordering of magnetic defects. The lines show simulated critical behaviour with different exponents in order to demonstrate that the decrease in frequency is too fast to correspond to higher order parameters such as that seen in 3D systems. Instead the best agreement is for a 2D Ising ferromagnet or antiferromagnet where β=0.125. The top inset shows a longitudinal field sweep at 30 K where the muon relaxation shows a decoupling of a component at approximately 109 G. The bottom inset shows a possible scenario resulting in stacking defects that may couple resulting in a 2D AF ordered state.

sites.

A possible physical description of the defects in $KTCNQF_4$, which may explain the 2D FM/AFM Ising behaviour, is shown schematically in the lower insert of Figure 5. In this model there is a plane of stacking faults, at which there will be $TCNQF_4$ which are not dimerised. It is these defects sites that may be able to interact within a 2D plane with a similar value of J, a measure of the magnetic exchange constant, leading to an ordering of defect magnetic moments. The 2D behaviour of this system is a curious result as the Ising model normally implies strong anisotropy from such mechanisms as strong spin-orbit coupling, but each $TCNQF_4^-$ radical has an orbitally quenched moment. Within TCNQ SP systems, although it can be thought of as a quasi 1D system where within a dimer the moments are antiferromagnetically coupled and the π-orbital overlap means that a molecular orbital is formed where the TCNQ dimer falls into a singlet, non-magnetic ground state but there will be singlet-triplet excitations. This may also be the same situation between TCNQ radicals located within the defect or structurally inhomogeneous regions, where π-orbital overlap is such that a molecular orbital is formed and a singlet ground state is also preferable. Avoided level crossing measurements on neutral TCNQ [36] have shown that the radical state

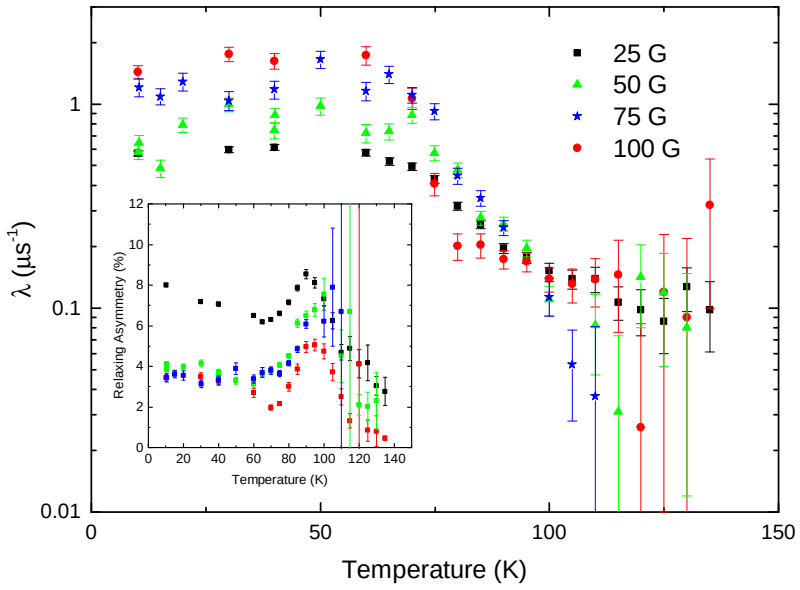

Figure 6. Temperature dependence of the muon relaxation rate in various longitudinal fields. *Inset:* Asymmetry of relaxing component showing a strong coupling to the changes in the relaxation.

has a strong anisotropy of the spin density at low temperatures that could alter the interactions between TCNQ radical in SP systems as well as within the defect. red Since the sample forms crystallites that are made of small needles, there may be a large amount of structural inhomogenities that could lead to various defects between stacks. Shifts in the stacking of different 1D columns of $TCNQF_4$ will also result in defects, as shown by the sketch in Figure 3, which could cause domain like behaviour that could propagate along the stack and would freeze at low temperatures.

To study the dynamics associated with the defect magnetism, temperature sweeps were collected in an applied longitudinal field up to 100 G. This should decouple any contributions from the F-μ^+-F states as well as decoupling the muon from any other nuclear moments (i.e. on ^{14}N). All data were fit using

$$G_{\mathrm{LF}}(t) = A_{\mathrm{LF}} \exp(-\lambda_{\mathrm{LF}} t) + A_{\mathrm{Bg}}, \tag{4}$$

where the subscript LF denotes that the relaxation is from the evolution of the muon polarisation in a longitudinal field. The raw data are shown within the supplementary information.

Application of a small (< 25 G) LF is normally enough to decouple muon-nuclear moment interactions and so the fact that a transition is still observed at 100 G LF is a good indication this behaviour is due to magnetic ordering. A small change can also be seen in the relaxing asymmetry shown in the inset of figure 6, with a peak being observed at around 90 K corresponding to the onset in the change in λ upon cooling. The relaxing asymmetry does not account for the full fraction of muons red and the peak is likely due to some of the muons responding to the internal fields associated with the defects. Well above the transition, the muons are no longer sensitive to the

dynamics of the defect phases as they are motionally narrowed and so less muons are relaxed by this component thus one may expect the relaxing asymmetry to decrease at higher T. Other muons that are not responding to these states may be too far from the local fields of the defects to detect changes in the orientation of their magnetic moments and so are easily repolarised accounting for both the flat baseline and other relaxation processes such as muon-fluorine interactions. It is no surprise however that the relaxing asymmetry decreases as the LF is increased, this is due to the larger field repolarising a larger, albeit relatively small, fraction of muons which is common in LF sweeps [29].

Although there have been suggestions that within these SP-type systems muon induced perturbations occur leading to paramagnetic defects [37, 38, 39], within our work, we see features in both the ESR and magnetic susceptibility measurements suggesting this effect is present regardless of the presence of a muon. However the fact that the percentage of the signal from the magnetic measurements and muon measurements related to the defect state is different, this may suggest that either; the magnetic measurements are giving an underestimate due to competition between magnetic responses, the muons preferentially stop near the defects as these could have a high amount of electron density associated with them although it can not be discounted that the muon may be able to perturb the environment promoting creation of a similar defect state that is observed in the magnetic data.

Conclusion

When the results from the ESR, magnetic susceptibility and μSR measurements are combined, it is clear that there is some deeper physics within this system that warrants further modelling and work in order to determine the physical origin of magnetically ordered defect states in $KTCNQF_4$. We have demonstrated that the temperature dependence of the muon precession frequency shows agreement with that of a 2D FM or AFM Ising model and have provided a reasonable scenario in which this might arise. Given the cusp in the magnetic susceptibility perhaps the AFM scenario is more likely. redHowever, this does pose the question of whether the system really is a 2D Ising AFM or or whether the magnetic transition is a result of the dimerisation of the defect spins and the critical scaling behaviour is related to the freezing out of singlet-triplet excitations associated with these defect dimer singlet-triplet excitations and that the freezing out of these excitations also show critical scaling behaviour? Further work should be conducted to confirm how these magnetic defects interact and the validity of our model. As the potential of charge-transfer compounds is becoming increasingly more apparent to the physics and chemistry communities, it is important to understand all of the underlying physics in order to optimise the creation of suitable compounds with technological use.

Acknowledgements

We would like to thank the Science and Technology Facilities Council for access to the muon spectrometers at the ISIS Neutron and Muon Source. AB would like to thank Durham University and the Australian National University for access to equipment to help conduct experiments.

References

[1] A. Brinkman, M. Huijben, M. Van Zalk, J. Huijben, U. Zeitler, J. C. Maan, W. G. Van Der Weil, G. Rijnders, D. H. A. Blank and H. Hilgenkamp. *Nat. Mat.* **6** (2007) 493
[2] Y. Murakami, K. Niitsu, T. Tanigaki, R. Kainuma, H. S. Park and D. Shindo. *Nat. Comm.* **5** (2014) 1
[3] W. Hu, Y. Liu, R. L. Withers, T. J. Frankcombe, L. Norén, A. Snashall, M. Kitchin, P. Smith, B. Gong, H. Chen, J. Schiemer, F. Brink and J. Wong-Leung. *Nat. Mat.* **12** (2013) 821
[4] S. J. Blundell and F. L. Pratt. *J. Phys. :Condens. Matter* **16** (2004) R771
[5] J. S. Miller. *Chem. Soc. Revs.* **40** (2011) 3266
[6] J. S. Miller. (1993) *Extended Linear Chain Compounds: Volume 3.* Plenum press: New York and London.
[7] A. I. Buzdin and L.N. Bulaevskii. *Sov. Phys. Usp.* **23** (1980) 409
[8] J. G. Vegter, T. Hibma and J. Kommandeur. *Chem. Phys. Letts.* **3** (1969) 427
[9] Y. Takaoka and K. Motizuki. *J. Phys. Soc. Jpn.* **47** (1979) 1752
[10] R. J. J. Visser, S. Oostra, C. Vettier and J. Voiron. *Phys. Rev. B.* **28** (1983) 2074
[11] B. van Bodegom, B. C. Larson and H. A. Mook. *Phys. Rev. B.* **24** (1981) 1520
[12] B. W. Lovett, S. J. Blundell, F. L. Pratt, Th. Jestädt, W. Hayes, S. Tagaki and M. Kurmoo. *Phys. Rev. B.* **61** (2000) 12241
[13] A. Brau and J.-P. Farges. *Phys. Status Solidi (b).* **61** (1974) 257
[14] A. Brau and J.-P. Farges. *Phys. Letts.* **A41** (1972) 179
[15] M. Hase, I. Terasaki and K. Uchinokura. *Phys. Rev. Letts.* **70** (1993) 3651
[16] M. Hase, I. Terasaki, K. Uchinokura, M. Tokunaga, N. Miura and H. Obara. *Phys. Rev. B.* **48** (1993) 9616
[17] M. Braden, G. Wilkendorf, J. Lorenzana, M. Ain, G. J. McIntyre, M. Behruzi, G. Heger, G. Dhalenne, A. Revcolevschi. *Phys. Rev. B.* **54** (1996) 1105
[18] J. M. Law, C. Hoch, R. Glaum, I. Heinmaa, R. Stern, J. Kang, C. Lee, M.-H. Whangbo and R.K. Kremer. *Phys. Rev. B.* **83** (2011) 180414
[19] M. Isobe and Y. Ueda. *J. Phys. Soc. Jpn.* **65** (1996) 1178
[20] K. Uchinokura. *J. Phys. Condens. Matter.* **14** (2002) R195
[21] J. -G. Lussier, S. M. Coad, D. F. McMorrow and D. McK Paul. *J. Phys. Conden. Matter.* **7** (1995) L325
[22] K. Manabe, H. Ishimoto, N. Koide, Y. Sadago and K. Uchinokura. *Phys. Rev. B.* **58** (1998) R575
[23] M. Hase, I. Terasaki, Y. Sasago, K. Uchinokura and H. Obara. *Phys. Rev. Letts***71** (1993) 4059
[24] S. B. Oseroff, S-W. Cheong, B. Aktas, M. F. Hundley, Z. Fisk and L. W. Rupp, Jr. *Phys. Rev. Letts.* **74** (1995) 1450
[25] Y. Lépine, A. Caillé and V. Larochelle. *Phys. Rev. B.* **18** (1978) 3585
[26] M. Konno, T. Ishii and Y. Saito. *Acta Cryst.* **B33** (1977) 763
[27] A. Berlie, I. Terry, S. R. Giblin and M. Szablewski. *Phys. Rev. B.* **93** (2016) 054422
[28] V. N. Glazkov, A. I. Smirnov, O. A. Petrenko, D. McK Paul, A.G.Vetkin and R. M. Eremina. *J. Phys.: Condens. Matter.* **10** (1998) 7879
[29] S.l. Lee, S. H. Kilcoyne, R. Cywinski. Muon Science: Muons in Physics, Chemistry and Materials. (1998) *Institute of Physics Publishing, UK*

[30] A. Schenck and F. W. Gygax in *Handbook of Magnetic Materials* **9**, ed. K. H. J. Buschow (1995, Elsevier, Amsterdam)
[31] A. I. Smirnov, V. N. Glazkov, L. I. Leonyuk, A.G.Vetkin and R. M. Eremina. *J. Exp. Theor. Phys.* **87** (1998) 1019
[32] J. H. Brewer, S. R. Kreitzman, D. R. Noakes, E. J. Ansaldo, D. R. Harshman and R. Keitel. *Phys. Rev. B.* **33** (1986) 7813
[33] T. Lancaster, S. J. Blundell, P. J. Baker, M. L. Brooks, W. Hayes, F. L. Pratt, J. L. Manson, M. M. Conner and J. A. Schlueter. *Phys. Rev. Letts.* **99** (2007) 267601
[34] D. A. Dixon, J. C. Calabrese and J. S. Miller. *J. Phys. Chem.* **93** (1989) 2284
[35] F. L. Pratt, T. Lancaster, P. J. Baker, S. J. Blundell, W. Kaneko, M. Ohba, S. Kitagawa, S. Ohira-Kawamura and S. Takagi. *Physica B.* **404** (2009) 585
[36] F. L. Pratt, S. J. Blundell, Th. Jestädt, B. W. Lovett, R. M. Macrae and W. Hayes. *Mag. Reson. Chem.* **38** (2000) S27
[37] S. Nakajima, T. Suzuki, Y. Ishi, J. Ohishi, I. Watanabe, T. Goto, A. Oosawa, N. Yoneyama, N. Kobayashi, F. L. Pratt and T. Saski. *J. Phys. Jpn. Soc.* **81** (2012) 063706
[38] W. Higemoto, H. Tanaka, I. Watanabe and K. Nagamine. *Phys. Letts. A.* **243** (1998) 80
[39] T. Suzuki, I. Watanabe, F. Yamada, Y. Ishii, K. Ohishi, T. Goto and H. Tanaka. *J. Phys.: Conf. Ser.* **502** (2014) 012041